

See discussions, stats, and author profiles for this publication at: <https://www.researchgate.net/publication/5233176>

# Resonance Raman Spectra and Raman Excitation Profiles of Rhodamine 6G from Time-Dependent Density Functional Theory

ARTICLE *in* CHEMPHYSCHEM · AUGUST 2008

Impact Factor: 3.42 · DOI: 10.1002/cphc.200800253 · Source: PubMed

---

CITATIONS

23

---

READS

53

## 2 AUTHORS:



**Julien Guthmuller**

Gdansk University of Technology

48 PUBLICATIONS 624 CITATIONS

SEE PROFILE



**Benoît Champagne**

University of Namur

401 PUBLICATIONS 8,733 CITATIONS

SEE PROFILE

# Resonance Raman Spectra and Raman Excitation Profiles of Rhodamine 6G from Time-Dependent Density Functional Theory

Julien Guthmuller\* and Benoît Champagne<sup>[a]</sup>

In a recent work, Shim et al.<sup>[1]</sup> reported well-resolved resonance Raman (RR) spectra of rhodamine 6G (R6G) using femtosecond stimulated Raman spectroscopy (FSRS). This technique presents the advantage of being able to acquire and quantify the RR cross-sections even in the presence of strong fluorescence<sup>[2]</sup> and therefore it extracts accurate Franck–Condon factors and, subsequently, ground-to-excited state geometry changes.<sup>[3]</sup> At the same time, though independently, the vibronic theory of RR spectroscopy was combined with time-dependent density functional theory (TDDFT) quantum chemical calculations to simulate and interpret the RR spectra of R6G.<sup>[4]</sup> Although a good agreement with experiment was generally obtained for both absorption and RR spectra, the comparison remains partly unsatisfactory because experimental RR spectra were either obtained using surface-enhanced resonance Raman spectroscopy (SERRS)<sup>[5–6]</sup> or for an excitation located in the vibronic shoulder of the absorption spectrum ( $\lambda = 488 \text{ nm}$ )<sup>[6]</sup> to reduce the fluorescence effects. Therefore, the publication of ref. [1] provides an impetus to extend herein our previous theoretical investigations to RR spectra recorded at other excitation wavelengths, to the concomitant RR excitation profiles, and to the dimensionless ground-to-excited state  $\Delta$ . The later aspect is also expected to give an insight concerning the relevance of the models employed for rationalizing and deducing the geometrical structure of the excited state.<sup>[3]</sup>

Figure 1 presents the theoretical RR spectra of R6G evaluated for excitations wavelengths at 532 and 555 nm as well as the experimental spectra recorded for the same wavelengths by Shim et al.<sup>[1]</sup> in methanol solutions. The two wavelengths correspond to excitations in resonance with the absorption maximum (of the first excited state) or located in the pre-resonant domain, respectively. The calculated spectra were determined following ref. [4], that is, considering the less polar ethanol solvent but, as shown in ref. [4], solvent effects on the vibrational frequencies, absorption spectrum, and RR spectrum in resonance with the first excited state are very small. A close agreement is found between theory and experiment in the 500–1800  $\text{cm}^{-1}$  energy domain. All experimental bands are reproduced by the theory and display quite comparable relative intensities. However, the simulations predict additional bands having small intensities. First, a band around 1420  $\text{cm}^{-1}$  determined by the TDDFT calculations is absent from the FSRS spectrum of ref. [1] while bands close to this energy were observed

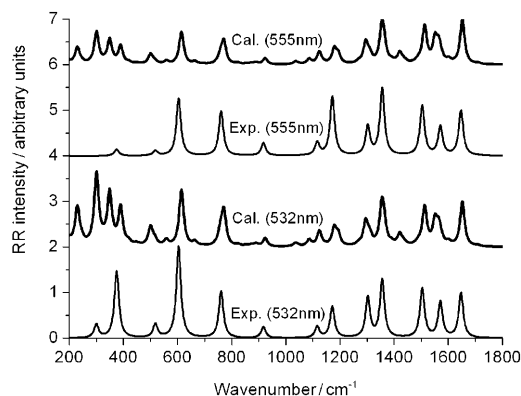


**Figure 1.** Comparison between theoretical and experimental RR spectra of R6G in resonance with the  $S_0 \rightarrow S_1$  transition. The experimental spectra are constructed from the experimental cross-sections reported in Table 1 and in the Supporting information of ref. [1].

in the spectrum reported by Watanabe et al.<sup>[6]</sup> Then, the two weak bands predicted between 1000 and 1100  $\text{cm}^{-1}$  are probably not evidenced in ref. [1] because they coincide with and were hidden by the CO stretch band of methanol at 1020  $\text{cm}^{-1}$ . Finally, two low frequency bands at 664 and 558  $\text{cm}^{-1}$  are obtained in the simulation and are also present in the FSRS experimental spectrum.<sup>[1]</sup> The main differences with respect to our previous comparison<sup>[4]</sup> with the spectrum of Watanabe et al.<sup>[6]</sup> is an improvement of the agreement for the two bands at 1513 and 1551  $\text{cm}^{-1}$ . Furthermore, the simulations (Figure 1) predict an increase of the low frequency bands for an excitation getting closer to the maximum of absorption. The enhancement found for the two modes at 614 and 771  $\text{cm}^{-1}$  is in agreement with experiment and confirms that this effect originates from a vibronic coupling mechanism since it is not accounted for using the short-time approximation.<sup>[4,7]</sup> It further shows also that a description of the vibronic structure is mandatory in order to correctly predict the RR spectrum of R6G in resonance with the first excited state in the region of 500–1800  $\text{cm}^{-1}$ . Nevertheless, there remains some disagreement with the FSRS results for the bands below 500  $\text{cm}^{-1}$ . These bands correspond to vibrations with dominant torsional motions and are less accurately described within the harmonic approximation.

An assignment of the experimental vibrational frequencies is proposed in Table 1. The differences between the calculated and measured vibrational frequencies are at the most 10  $\text{cm}^{-1}$ . The values of  $\Delta_i$  are displayed in Table 1 in order to compare our theoretical results to the RR intensity analysis performed by Shim et al.<sup>[1]</sup> The  $\Delta$  values describe the geometrical modifications along the vibrational normal coordinates occurring upon excitation to the (first) excited state and contain there-

[a] Dr. J. Guthmuller, Dr. B. Champagne  
Laboratoire de Chimie Théorique Appliquée  
Faculté Universitaire Notre-Dame de la Paix  
Rue de Bruxelles 61, 5000 Namur (Belgium)  
Fax: (+32)81 724567  
E-mail: julien.guthmuller@fundp.ac.be

**Table 1.** Assignment of the vibrational bands of R6G.

Theory <sup>[a]</sup> Frequency [cm <sup>-1</sup> ]	$\Delta_i$	Experiment <sup>[b]</sup> Frequency [cm <sup>-1</sup> ]	$\Delta_i$
230	0.33	–	–
301	0.38	300	0.24
349	–0.29	375	0.46
390	0.24		
500	–0.15	518	0.17
516	<b>0.08</b>		
558	0.08	–	–
614	–0.24	604	0.42
664	–0.06	–	–
759	–0.11	761	0.29
771	–0.17		
924	0.08	917	0.14
1036	0.05	–	–
1087	0.07	–	–
1124	–0.11	1116	0.15
1179	<b>0.12</b>	1172	0.24
1194	–0.09		
1295	<b>0.13</b>		
1301	–0.04	1303	0.28
1310	<b>0.08</b>		
1354	<b>0.17</b>	1356	0.34
1363	–0.12		
1421	0.09	–	–
1433	0.04	–	–
1442	–0.03	–	–
1513	–0.17	1504	0.32
1551	<b>0.14</b>	1571	0.27
1565	<b>0.12</b>		
1576	–0.05		
1602	–0.05	–	–
1652	0.19	1647	0.30

[a] Multiple theoretical frequencies assigned to a single experimental band are grouped in bold. [b] The experimental results are taken from reference [1] and only produce the absolute value of the  $\Delta$ s.

fore information on the geometrical structure of the excited state. Analysis of Table 1 leads to the following observations: 1) experimental bands (see also Figure 1) at 518, 761, 1172, 1303, 1356 and 1571 cm<sup>-1</sup> are assigned to a superposition of two or three different vibrational modes. Indeed, in these spectral regions characterized by a single band, quantum-chemical calculations predict several modes of similar frequencies and non-negligible  $\Delta$  values, suggesting therefore that geometrical modifications along various normal coordinates are responsible for the RR intensities of these bands; 2) even after accounting for the superposition of transitions, the  $\Delta$ s values obtained with both approaches present comparable absolute amplitudes; 3) the TDDFT  $\Delta$ s are generally smaller than the  $\Delta$ s deduced from experiment [for instance, for the band at 604 cm<sup>-1</sup> this is directly related to its larger relative RR intensity

(Figure 1)]; and 4) the calculated  $\Delta$ s for the vibrational modes at 349 and 390 cm<sup>-1</sup> suggest that the intense band at 375 cm<sup>-1</sup> in the experiment at 532 nm arises from a linear combination of these two vibrations.

The poorly accurate intensity found for the band at 301 cm<sup>-1</sup> as well as the presence of an additional band at 230 cm<sup>-1</sup> demonstrate the limitations of the quantum chemical approach. Indeed, despite treating the vibronic and solvent effects and using an efficient combination of XC functional (using BHandHLYP does not change the conclusion) and basis set, part of the low-frequency experimental spectra cannot be reproduced. Since this is associated with low-frequency torsional motions, one can suggest the discrepancy originates from the lack of anharmonicity treatment, currently out of reach for R6G with such quantum-chemical approaches. Moreover, specific hydrogen bonding with the solvent as well as experimental reasons cannot be excluded as an explanation for this discrepancy.

In order to compare with the results presented in ref. [1], Figure 2 presents the excitation profiles for the five representative bands at 614, 759+771, 1179+1194, 1354+1363, and 1652 cm<sup>-1</sup>, which were assigned to the experimental bands at 604, 761, 1172, 1356, and 1647 cm<sup>-1</sup>, respectively. The simulation of the excitation profiles for the bands involving more than one vibrational coordinate was realised by summing the RR intensities of the contributing modes. The low-frequency modes present a simple bell-shape structure, whereas the modes at higher frequencies display two peaks. The shapes of the excitation profiles are directly connected to the vibronic structure of the absorption spectrum while they illustrate the

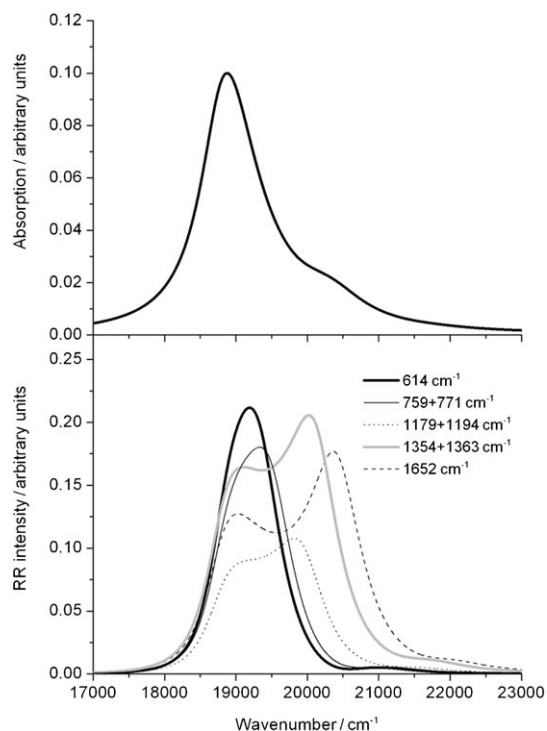


**Figure 2.** Top: Absorption spectrum of R6G; Bottom: RR excitation profiles of R6G for five bands. The results are calculated at the TDDFT/B3LYP/6-311G\*/IEFPCM level of approximation.

impact of the excitation wavelength. Thus, the two low frequency bands at 614 and 759+771 cm<sup>-1</sup> are strongly enhanced for an excitation at the maximum of absorption (~18800 cm<sup>-1</sup>). The simulated excitation profiles are also in general good agreement with the one reported in ref. [1]. The main differences concern the relative intensities, following the differences in the  $\Delta$  values of Table 1. Other differences predominantly arise from the use of a smaller damping factor in the TDDFT-based simulations as well as from the neglect of inhomogeneous broadening.<sup>[8]</sup>

In summary, the vibronic theory of RR spectroscopy was combined with TDDFT quantum-chemical calculations to assess the latest FSRs results on R6G<sup>[1]</sup>, that is, the RR spectra for excitation wavelengths corresponding to the absorption maximum, the RR excitation profiles, and the dimensionless ground-to-excited state  $\Delta$ s. The agreement with experiment is found to be very good, which enables to fully address the contributing vibrational bands and to demonstrate that several bands originate from two or three vibrational normal-mode contributions. These comparisons also substantiate the use of the vibronic theory to reproduce the relative RR intensities of several low- and high-frequency bands whereas they suggest that anharmonicity corrections might be important in the 200–500 cm<sup>-1</sup> region. Moreover, simulated RR excitation profiles quantify the impact of the excitation wavelength.

## Computational Methods

The RR intensities were calculated using the vibronic theory expressions of RR scattering derived by Peticolas and Rush<sup>[9]</sup> assuming independent displaced harmonic oscillators. The RR intensity for the fundamental 0 → 1<sub>i</sub> transition is given by Equation (1)

$$I_{0 \rightarrow 1}(\omega_L) \propto \omega_L(\omega_L - \omega_i)^3 \frac{\Delta_i^2}{2} |\Phi(\omega_L) - \Phi(\omega_L - \omega_i)|^2 \quad (1)$$

where  $\omega_L$  is the frequency of the incident light,  $\omega_i$  is the frequency of the  $i$ th vibrational normal mode,  $\Delta_i$  is the dimensionless displacement along the  $i$ th normal coordinate, and the function  $\Phi(\omega_L)$  depends on the vibrational frequencies, the origin transition energy  $\omega_{e0,g0}$ , the Franck-Condon factors, as well as on a damping factor  $\Gamma$  describing a homogeneous broadening. In order to reproduce the experimental  $\lambda_{\text{max}}$  (530 nm) and the broadening of the absorption spectrum, values of 18800 cm<sup>-1</sup> and 400 cm<sup>-1</sup> have been taken for  $\omega_{e0,g0}$  and  $\Gamma$ , respectively. The geometrical displacements  $\Delta_i$  between the ground and excited states potential minima were evaluated from the partial derivatives of the excited-state electronic energy along the vibrational normal coordinates at the ground-state equilibrium position. The theoretical and experimental RR spectra presented in Figure 1 were obtained by applying a Lorentzian function with a FWHM of 20 cm<sup>-1</sup> on the calculated intensities and experimental cross-sections of Shim et al.<sup>[1]</sup> Additionally, these spectra were normalized so that the intensity of the band close to 1650 cm<sup>-1</sup> is equal to unity. The geometries and frequencies of vibration in the ground state were obtained by means of density functional theory at the B3LYP/6-311G\* level of theory. The vertical excitation energies, necessary to evaluate the displacements  $\Delta_i$ , were calculated using TDDFT with the same functional and basis set. The effect of the solvent was taken into account by employing the integral equation formalism of the polarizable continuum model.<sup>[10]</sup> Finally, the theoretical vibrational normal-mode

frequencies were corrected using a scaling factor of 0.98 in order to take into account anharmonicity effects and errors arising from the theoretical method.<sup>[11]</sup> All quantum-chemical calculations were carried out using the GAUSSIAN 03 program<sup>[12]</sup> and were coupled to a homemade program to simulate the RR spectra. Further details about the calculation of RR intensities and absorption spectra can be found elsewhere.<sup>[4,13]</sup>

## Acknowledgements

The authors thank Sangdeok Shim, Christina M. Stuart and Richard A. Mathies for providing experimental data to plot Figure 1. J.G. thanks the Fund for Scientific Research F.R.S.-FNRS for his postdoctoral grant under the convention No. 2.4.509.04.F. B.C. thanks the F.R.S.-FNRS for his research director position. The calculations have been performed on the Interuniversity Scientific Computing Facility (ISCF) installed at the Facultés Universitaires Notre-Dame de la Paix (Namur, Belgium) for which the authors gratefully acknowledge the financial support of the F.R.S.-FRFC and the Loterie Nationale for the convention No. 2.4578.02, and of the FUNDP.

**Keywords:** density functional calculations • resonant Raman spectroscopy • rhodamine 6G • vibrational spectroscopy • vibronic coupling

- [1] S. Shim, C. M. Stuart, R. A. Mathies, *ChemPhysChem* **2008**, *9*, 697–699.
- [2] D. W. McCamant, P. Kukura, S. Yoon, R. A. Mathies, *Rev. Sci. Instrum.* **2004**, *75*, 4971–4980.
- [3] a) E. J. Heller, R. L. Sundberg, D. Tannor, *J. Phys. Chem.* **1982**, *86*, 1822–1833; b) A. B. Myers, *Chem. Rev.* **1996**, *96*, 911–926; c) A. B. Myers, *Acc. Chem. Res.* **1997**, *30*, 519–527.
- [4] J. Guthmuller, B. Champagne, *J. Phys. Chem. A* **2008**, *112*, 3215–3223.
- [5] a) P. Hildebrandt, M. Stockburger, *J. Phys. Chem.* **1984**, *88*, 5935–5944; b) A. M. Michaels, M. Nirmal, L. E. Brus, *J. Am. Chem. Soc.* **1999**, *121*, 9932–9939.
- [6] H. Watanabe, N. Hayazawa, Y. Inouye, S. Kawata, *J. Phys. Chem. B* **2005**, *109*, 5012–5020.
- [7] L. Jensen, G. C. Schatz, *J. Phys. Chem. A* **2006**, *110*, 5973–5977.
- [8] M. Lilenko, D. Tittelbach-Helmrich, J. W. Verhoeven, I. R. Gould, A. B. Myers, *J. Chem. Phys.* **1998**, *109*, 10958–10969.
- [9] a) W. L. Peticolas, T. Rush III, *J. Comput. Chem.* **1995**, *16*, 1261–1270; b) T. Rush III, R. Kumble, A. Mukherjee, M. E. Blackwood Jr., T. G. Spiro, *J. Phys. Chem.* **1996**, *100*, 12076–12085.
- [10] J. Tomasi, B. Mennucci, R. Cammi, *Chem. Rev.* **2005**, *105*, 2999–3093.
- [11] J. P. Merrick, D. Moran, L. Radom, *J. Phys. Chem. A* **2007**, *111*, 11683–11700.
- [12] *Gaussian 03, Revision C.02*, M. J. Frisch, G. W. Trucks, H. B. Schlegel, G. E. Scuseria, M. A. Robb, J. R. Cheeseman, V. G. Zakrzewski, J. A. Montgomery, R. E. Stratmann, J. C. Burant, S. Dapprich, J. M. Millam, A. D. Daniels, K. N. Kudin, M. C. Strain, O. Farkas, J. Tomasi, V. Barone, M. Cossi, R. Cammi, B. Mennucci, C. Pomelli, C. Adamo, S. Clifford, J. Ochterski, G. A. Petersson, P. Y. Ayala, Q. Cui, K. Morokuma, D. K. Malick, A. D. Rabuck, K. Raghavachari, J. B. Foresman, J. Cioslowski, J. V. Ortiz, A. G. Baboul, B. B. Stefanov, G. Liu, A. Liashenko, P. Piskorz, I. Komaromi, R. Gomperts, R. L. Martin, D. J. Fox, T. Keith, M. A. Al-Laham, C. Y. Peng, A. Nanayakkara, M. Challacombe, P. M. W. Gill, B. G. Johnson, W. Chen, M. W. Wong, J. L. Andres, C. Gonzalez, M. Head-Gordon, E. S. Replogle, J. A. Pople, Gaussian, Inc., Wallingford CT, **2004**.
- [13] J. Guthmuller, B. Champagne, *J. Chem. Phys.* **2007**, *127*, 164507.

Received: April 25, 2008

Revised: June 20, 2008

Published online on July 10, 2008